Unusual magnetic transitions and nature of magnetic resonance spectra in oxide glasses containing gadolinium

Janis Kliava
CPMOH, UMR 5798 CNRS-Université Bordeaux-I, 33405 Talence cedex, France

Alexander Malakhovskii
Department of Chemistry, Bar-Ilan University, Ramat-Gan 52900, Israel

Irina Edelman,* Anatoly Potseluyko, Eleonora Petrakovskaja, and Svetlana Melnikova
L. V. Kirensky Institute of Physics SB RAS, Krasnoyarsk 660036, Russia

Tat'jana Zarubina and Gurii Petrovskii
S. V. Vavilov State Optical Institute, St. Petersburg 199034, Russia

Yishay Bruckental and Yosef Yeshurun
Department of Physics, Bar-Ilan University, Ramat-Gan 52900, Israel
(Received 11 November 2004; revised manuscript received 21 December 2004; published 8 March 2005)

Magnetic susceptibility, electron paramagnetic resonance (EPR), and optical properties have been studied in a glass system $\{20La_2O_3-22Al_2O_3-23B_2O_3-35(SiO_2+GeO_2)\}$ with a part of La_2O_3 substituted by Gd_2O_3 in different concentrations. Positive Weiss constants have been found in the more heavily doped glasses and ascribed to clustering of Gd^{3+} ions. Two magnetic phase transitions at 55 and 12 K were detected and ascribed, respectively, to ferromagnetic and antiferromagnetic clusters containing Gd ions. The overall shape of the EPR spectra shows the presence of clustering at the higher Gd contents. At low temperatures the cluster-related resonance signal is altered in shape, indicating an onset of magnetic anisotropy field. This signal is convincingly fitted to superparamagnetic resonance arising from ferromagnetic nanoparticles. The clustering, depending on the Gd concentration, correlates with a significant shift to lower energies of the strong optical absorption band edge, ascribed to a charge transfer transition between Gd ions. A nonmonotonous change of refractive index with the increase of the Gd content indicates changes in the glass matrix and in Gd cluster structure.

DOI: 10.1103/PhysRevB.71.104406 PACS number(s): 75.70.Cn, 75.20.−g, 76.30.Kg, 78.66.Jg

I. INTRODUCTION

Magnetic ordering in compounds containing gadolinium—both stoichiometric crystals and glasses activated by this rare earth element—attracts much attention owing to magnetic and optical properties of these materials promising for technical applications (e.g., see Refs. 1–10). Gadolinium most frequently occurs in the Gd^{3+} state with electronic configuration $4f^7$ and the ground state $^8S_{7/2}$; owing to the absence of orbital moment this ion is particularly well adapted to magnetic resonance experiments. Various magnetic ordering types, including noncolinear amplitude-modulated antiferromagnetic order, have been observed in Gd compounds and discussed in the literature.[1] Meanwhile, dielectric oxide Gd compounds were shown to have a colinear antiferromagnetic order at low temperatures; for example, Gd_2O_3 used as a starting material in the glass synthesis has a Weiss constant[2] of -13 K. Polarized neutron experiments[3] have shown different low-temperature ($T<10$ K) dependencies of the contribution to the magnetic susceptibility χ of the Gd^{3+} ion in two different crystallographic positions in cubic Gd_2O_3: $C_{3i}(\chi_1)$ and $C_2(\chi_2)$. Below 10 K the two contributions diverge quite rapidly, and at 1.8 K χ_1 is larger than χ_2 by a factor of about 9. However, the average susceptibility is in good agreement with earlier results obtained from the magnetization measurement.[2] In order to account for this behavior, the authors of Ref. 3 assume that the ions in C_2 positions have a strong tendency to form antiferromagnetic clusters, thus reducing their contribution to the susceptibility. Gd clustering was studied in diluted magnetic compounds $Lu_{2-x}Gd_xO_3$,[4] and antiferromagnetic order at low temperatures was shown to occur in this case as well. Several oxide glass systems containing gadolinium were studied using electron paramagnetic resonance (EPR) and magnetic measurements. Temperature dependence of magnetization was studied in Ref. 5 for the glass compositions $\{(100-x)[4Bi_2O_3\cdot PbO)]-xGd_2O_3\}$ and $\{(100-x)[3Bi_2O_3\cdot 2PbO)]-xGd_2O_3\}$ with $x=1$, 5, 10, and 20 mole %. The magnetization of these glasses follows the Curie-Weiss law, and the paramagnetic Curie temperature (Θ_p) is 0 for $x=1$ mole % and changes from -15.2 to -34.2 K for higher x values. The magnetic moment per Gd^{3+} ion ($x=1$) is lower than for the free Gd^{3+} ion and further decreases as x increases. These results were explained by a formation of ion pairs coupled by superexchange interaction. Because of rigidity of the lead-bismuth matrix, at high bismuth content an unusually high fraction of Gd^{3+} ions is supposedly located in sites with high crystal field and low coordination number. A similar situation was found in glasses of compositions $\{xGd_2O_3(1-x)(3B_2O_3PbO)\}$,[6] $\{xGd_2O_3(1$

$-x)(Na_2OB_2O_3)\}$,[7,8] $\{xGd_2O_3(1-x)(Na_2B_4O_7)\}$,[9] and $\{Bi_2O_3GeO_2Gd_2O_3\}$.[10] In all cases $\Theta_p=0$ for $x=1$–2 mole % (depending on the glass composition) and becomes negative for higher x. The absolute value of Θ_p increases with the increase of x and depends on the glass composition.

Magnetic properties of Gd compounds depend on the structure of the environment of the Gd^{3+} ions and are strongly influenced by clustering. The vitreous state provides an additional "degree of freedom" for these conditions. Recently, we have revealed[11] *ferromagnetic clustering* of Gd^{3+} in the glass system $\{xGd_2O_3-(1-x)(La_2O_3-Al_2O_3-B_2O_3-SiO_2-GeO_2)\}$. Since this is quite an unusual phenomenon, we have carried out a more comprehensive study with the aim of elucidating the nature of the magnetic state of the Gd^{3+} clusters. This paper focuses on magnetic (static and magnetic resonance) and optical (strong optical absorption band edge) characterization of low-temperature magnetic phase transitions arising at low temperatures in this system.

II. EXPERIMENT

The glasses were prepared from the mixture of Gd_2O_3, La_2O_3, Al_2O_3, H_3BO_3, SiO_2, and GeO_2 with the technology described in Ref. 11. The impurity contents did not exceed 5×10^{-3} mass % for Fe (in Al_2O_3), 5×10^{-4} mass % for Ce (in La_2O_3), 10^{-4} mass % for other impurities. Four samples, Gd1, Gd2, Gd3, and Gd4, were synthesized with, respectively, 0.1, 1.0, 5.0, and 10 mass % of Gd_2O_3 substituting the equivalent amounts of La_2O_3. For such substituting, the environment of the Gd^{3+} ions is expected to remain unchanged when the Gd_2O_3 content increases.

The magnetization was measured as a function of temperature (5–300 K) and magnetic field (0–5 tesla) using a Quantum Design MPMS-XL superconducting quantum interference device magnetometery with a scan length of 4 cm. The relative errors in the magnetization values are lower than $\pm$ 0.01%. The EPR spectra were measured between 4.2 and 293 K in the X band (9.5 GHz) with a Bruker EMX spectrometer and in the Q band (35 GHz) with a Bruker ESP300 spectrometer. The optical absorption was measured at room temperature in the wavelength range of 210–500 nm with a UVICON 943 spectrophotometer. The refractive index was measured as a function of the wavelength from 450 to 650 nm at room temperature with the prism method.

III. RESULTS AND DISCUSSION

A. Magnetization

The field dependencies of the magnetization of the glasses at 5 K are shown in Fig. 1. Diamagnetic contribution of the glass matrix has been subtracted (see below). The magnetization curves of all glasses are very similar; meanwhile, some samples of the Gd4 glass (Gd') show weak features in the high-field range (Fig. 1).

Because of the absence of orbital moment and the half-integer spin ($S=7/2$), the effect of the crystal field (CF) on the magnetic moment of the Gd^{3+} ion is relatively small, and for an isolated ion the temperature dependence of the magnetization should follow the Curie law. However, the Gd ions

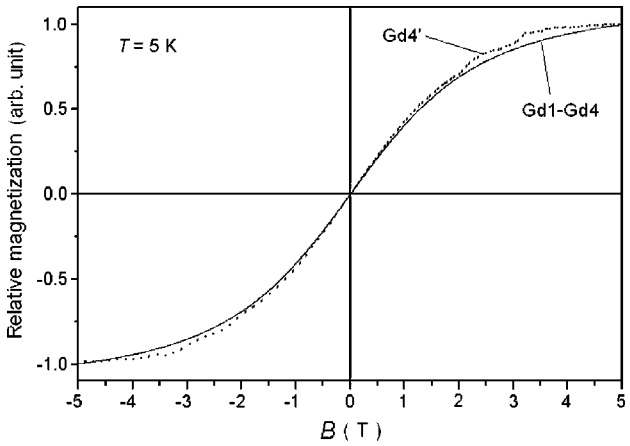

FIG. 1. Normalized magnetization of Gd1–Gd4 glasses versus magnetic field, measured at 5 K.

can form clusters, so that the magnetic susceptibility of these glasses in the paramagnetic region ($T>|\Theta|$) can be written in the form

$$\chi = a + C_i/T + C_c/(T-\Theta), \tag{1}$$

where

$$C_i = n_i m_i^2/3k, \quad C_c = n_c m_c^2/3k, \tag{2}$$

and n and m are defined below.

The terms in Eq. (1) account, respectively, for the diamagnetic susceptibility, the isolated paramagnetic ions, and the Gd in clusters. All terms in Eq. (1), the diamagnetic term included, are given per kg of gadolinium. C_i and C_c are the Curie constants for isolated and clustered Gd ions, n_i and n_c are, respectively, the numbers of the isolated and clustered Gd ions per kg of gadolinium; m_i and m_c are the corresponding high-temperature ($T\gg|\Theta|$) values of the magnetic moment, and Θ is the Weiss constant. The second term in Eq. (1) is valid for

$$\mu_B g_J JB \ll kT. \tag{3}$$

The susceptibility was measured in field $B=0.2$ T. Up to this field the magnetization is a linear function of B down to the lowest measurement temperature, $T=5$ K; see Fig. 1, implying that Eq. (3) is valid for the whole temperature range of the present study.

For the analysis of the experimental results it is more convenient to make use of the product $\chi T=aT+C_i+C_cT/(T-\Theta)$. For isolated Gd ions $C_c=0$ and χT is a linear function of temperature. The experimental temperature dependence of χT for Gd1, shown in Fig. 2, is perfectly linear, so one can infer that this glass contains only isolated Gd ions. From Fig. 2 we find the value of $a=-3.2$ A m^2 kg^{-1} T^{-1}. Assuming the diamagnetic susceptibility to be due to the glass matrix and taking into account the Gd concentrations in the glasses, we find the following values of a per kg of Gd: -0.32, -0.062, and -0.03 A m^2 kg^{-1} T^{-1}, respectively, for Gd2, Gd3, and Gd4. Next, we subtract the

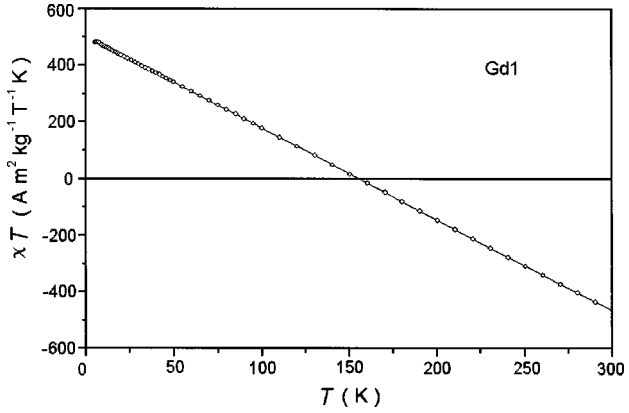

FIG. 2. Temperature dependence of the χT product for Gd1 in the magnetic field $B=0.2$ T.

diamagnetic contribution from the experimental susceptibilities of all glasses (see Fig. 3) and compare them with the function $(\chi-a)T$

$$(\chi - a)T = C_i + C_c T/(T - \Theta). \tag{4}$$

For a pure paramagnet (isolated ions) this function is a constant. One can see, in contrast, that the corresponding experimental dependencies in the glasses Gd2, Gd3, and Gd4 are very complex and show conspicuous well-defined peaks (Fig. 3). This behavior clearly indicates the existence of magnetically ordered clusters. This finding will be further corroborated by the results of EPR and optical measurements.

The shape of the feature at $T_1=55$ K (Fig. 3) is typical for the region of a ferromagnetic phase transition for some ferromagnets.[12,13] In the case of the ferromagnetic order, the Weiss constant is positive and the function Eq. (4) should decrease with increasing temperature above the ferromagnetic transition. This is in agreement with the experimental tendency above the feature at $T=55$ K (see Fig. 3). Note that anomalous dependence of Faraday rotation on doping concentration in Gd-doped germanate glasses, observed by Yuan and Chee,[14] was attributed to ferrimagnetic clusters. Ternary boride $Gd_{0.57}Rh_{3.43}B_2$ also reveals ferromagnetic ordering.[15]

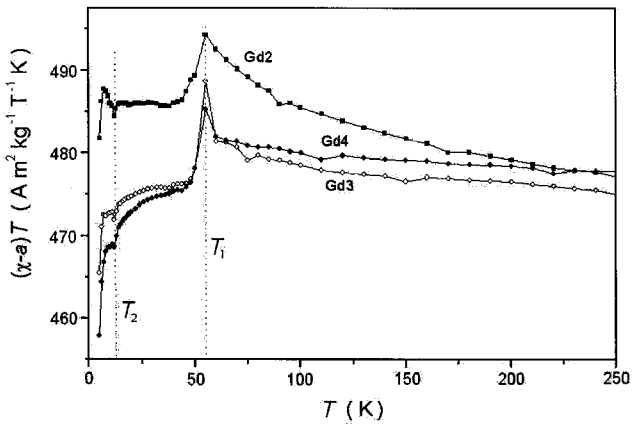

FIG. 3. Temperature dependence of $(\chi-a)T$ for Gd2–Gd4 in the magnetic field $B=0.2$ T.

At $T_2=12$ K one more peak in the $(\chi-a)T$ dependence is observed (Fig. 3). It can be related to magnetic or structural phase transition in the same clusters or in clusters of another structure. Indeed, even the gadolinium oxide can exist in two forms: cubic and monoclinic.[16] Complicated composition of the glass studied gives additional possibilities for different local structures, which strongly influence the exchange interaction between the Gd ions. The temperature of the magnetic ordering of clusters should increase with the size of the clusters up to the value typical for the bulk material at some critical size of the cluster.[17] Therefore, the observed narrow features at definite temperatures in Fig. 3 imply that there is a substantial amount of clusters above the critical size in the studied glasses.

When $T\rightarrow 0$ but the condition Eq. (4) is still fulfilled, even a small amount of isolated ions can make a substantial contribution to the magnetic susceptibility; see Eq. (1). The second term in Eq. (4) is no longer valid for $T<\Theta$. However, the susceptibility of disordered antiferromagnets and ferromagnets changes slowly in the low-temperature range, approaching some finite value when $T\rightarrow 0$.[12,13,18,19] Therefore $(\chi-a)T$ is approximately a linear function of T in the same region, and $(\chi-a)T\rightarrow C_i$ when $T\rightarrow 0$. In this way we can approximately estimate the parameter C_i. For the estimation we used only the first two points ($T=5$ and 6 K), because of the marked influence of the close phase transition at 12 K (see Fig. 3).

At high temperatures ($T\gg|\Theta|$)

$$(\chi - a)T \approx C_i + C_c(1 + \Theta/T) \tag{5}$$

is a linear function of 1/T and it approaches (C_i+C_c) when $1/T\rightarrow 0$. By extrapolating the experimental function $(\chi-a)T$, to zero value of 1/T, we find (C_i+C_c). From Eq. (2) it follows that

$$(C_i + C_c) = (m_i^2 n_i + m_c^2 n_c)/3k = m_{eff}^2 n/3k, \tag{6}$$

where $n=n_i+n_c$ is the total number of Gd ions per kg of gadolinium, and $m_i=m_c=m_{eff}$ is implicit. From Eq. (6) we can estimate the effective magnetic moments of Gd ions in the glasses. Measurements carried out on different samples of the same glass have shown a spread in the (C_i+C_c) values of about ± 8 %, obviously due to inhomogeneous distribution of the Gd^{3+} ions in the glasses. Correspondingly, m_{eff} of all the glasses was estimated as 7.7 μ_B with accuracy of ± 4 % (since the Curie constant is proportional to the square of the magnetic moment). This corresponds to the magnetic moment of Gd in Gd_2O_3.[2] The magnetic moment of a free-Gd ion, $\mu_B g_J[J+(J+1)]^{1/2}$, is 7.95 μ_B. If one neglects the difference between the magnetic moments of isolated and clustered Gd ions, the ratio $K=C_c/(C_i+C_c)\approx n_c/(n_i+n_c)$ will characterize the degree of clustering in the glasses. The estimated values of K are quoted in Table I.

A linear extrapolation of the inverse susceptibility corrected for the diamagnetic term, $1/(\chi-a)$, carried out in the region of 130–300 K gives the "pseudo-Weiss" constants, Θ_1 (see Table I). If the contribution of isolated ions is taken into consideration according to Eq. (4), the true Weiss constants of the clusters, Θ_2, should be larger.[20] Now, knowing the

TABLE I. Contents of gadolinium oxide, Weiss constants, and estimates of the clustering degree in the glasses (susceptibility data).

	Gd1	Gd2	Gd3	Gd4
Gd_2O_3 (mass %)	0.1	1.0	5.0	10.0
Θ_1 (K)	0	+3.0	+1.4	+0.9
Θ_2 (K)	0	+50±5	+12±2	+9±2
K (%)	0	⩽3	⩽8	⩽10

parameters C_i and C_c, we can substitute the experimental values of $(\chi - a)T$ from Fig. 3 at any $T > |\Theta|$ into Eq. (4) and determine Weiss constants of the clusters (Table I). The Weiss constant of clusters in Gd2 is substantially larger than that in Gd3 and Gd4. This fact corresponds to the above interpretation of T_1 and T_2 as indicating two types of clusters with different magnetic ordering. In particular, we can assume that in Gd2 the clusters with ferromagnetic ordering at 55 K prevail. The degree of clustering in Gd3 and Gd4 is much larger than in Gd2, but Weiss constants are much smaller than in Gd2. This means that in Gd3 and Gd4 the relative number of clusters with the low temperature of ordering increases.

B. EPR

Preliminary data on the room temperature EPR spectra in these glasses have been reported previously.[11] In cooling down to the liquid nitrogen temperature the spectra remain nearly the same. More pronounced changes in the shape of the spectra are observed below approximately 60 K. Figure 4 shows a comparison between the EPR spectra at room and liquid helium temperatures. The overall spectra shapes in the Gd1–Gd4 samples belong to the so-called "*U*-spectrum" (from *ubiquitous*) type.[6,7,10,21–23] In the corresponding *Q*-band spectra only a relatively narrow single line with $g_{eff} = 2.0$ is observed.

In the EPR spectra of Gd2 in comparison with the Gd1 glass, only a slight line broadening is observed. On the other hand, in the Gd3 and Gd4 glasses all spectral features are broadened. This broadening is naturally ascribed to dipole-dipole interaction between the Gd^{3+} ions. Meanwhile, in order to unambiguously account for the spectra transformation with the gadolinium concentration, a more quantitative analysis is needed.

Previously, we have numerically simulated the EPR spectra of the glasses by means of an *ab initio* code[11,24] directly relating the atomic positions in the environment of the paramagnetic ions to the spin-Hamiltonian parameters using the superposition model. A more detailed account of these results will be published elsewhere. In the context of the present study, we recall here that clustering of the Gd^{3+} ions has been clearly evidenced in Ref. 11; indeed, the EPR spectra in more heavily doped glasses have been accounted for as superposition of two distinct signals, arising from ions (i) diluted in the glass matrix and (ii) included in clusters.

In this paper, we put forward another approach based on a numerical analysis of *experimental* EPR spectra. The theoretical background for this transformation is as follows. For an isolated paramagnetic center (ion or structure defect) embedded in a disordered matrix (glass), the various spin-Hamiltonian parameters and orientation angles are considered as components of a random vector $\boldsymbol{X}$. A "generalized distribution density of the resonance magnetic field" is obtained as a convolution with a Dirac δ function of the resonance magnetic field B_r of an appropriate transition intensity $W(\boldsymbol{X})$ weighted by a multivariate distribution density $P(\boldsymbol{X})$[24,25]

$$\mathcal{J}(B_r) = \int P(\boldsymbol{X}) W(\boldsymbol{X}) \delta[B_r - B_r(\boldsymbol{X})] dV(\boldsymbol{X}). \tag{7}$$

$\mathcal{J}(B_r)$ features the EPR *absorption* spectrum at zero *intrinsic* linewidth in the absence of line broadening mechanisms *not related to the structural disorder* (e.g., dipole-dipole interaction or spin-lattice relaxation). In order to account for the spectra broadening, $\mathcal{J}(B_r)$ is convoluted with an appropriate line shape function $F(B - B_r, \Delta_B)$

$$\mathcal{P}(B) = \int \mathcal{J}(B_r) F(B - B_r, \Delta_B) dB_r. \tag{8}$$

Here, $F(B - B_R, \Delta_B)$ includes all broadening mechanisms other than orientational and structural disorder. By choosing it in the form of a derivative-of-absorption line shape, $\mathcal{P}(B)$ can be directly compared to the experimental EPR spectrum.

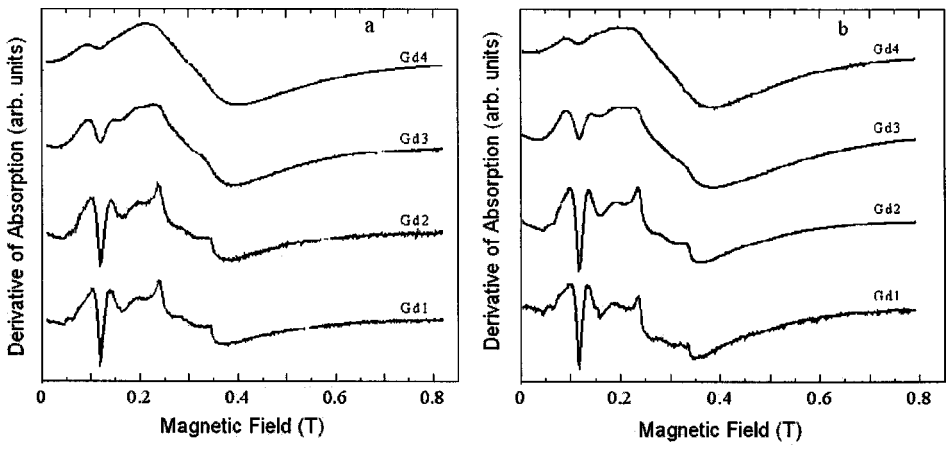

FIG. 4. Experimental *X*-band (9.45 GHz) EPR spectra at 300 (a) and 4.5 K (b).

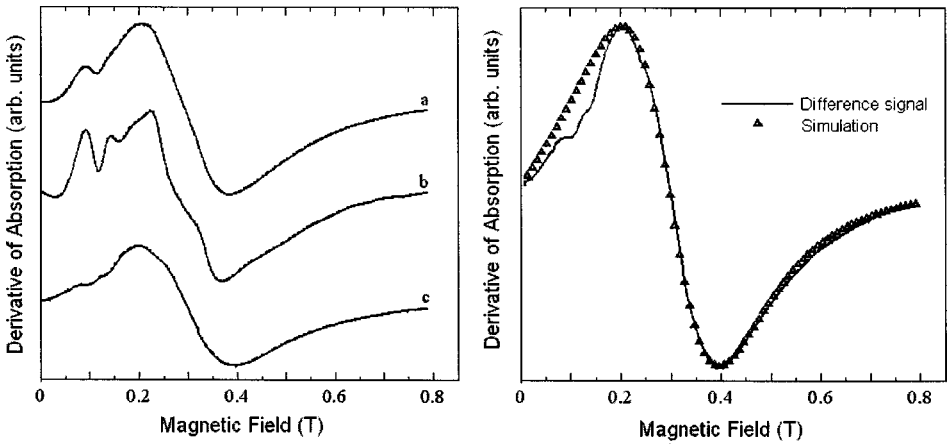

FIG. 5. Left: representation of the EPR spectrum of Gd4 at 300 K (a) as a linear combination of the room-temperature spectrum of Gd1 convoluted with the line shape Eq. (9) for $\Delta_B = 0.010$ T (b) and an underlying resonance: (c) $=$(a)-0.32 (b). Right: fitting to the curve (c) with the modified Bloch line shape for $B_0 = 0.30$ T and $\Delta_B = 0.010$ T.

Note that Eq. (8), in the form of a simple integral, requires an orientation-independent linewidth Δ_B. Only in this particular (but very often occurring in practice) case can the above two-stage approach be applied.

In his work[26] Van Vleck showed that for diluted paramagnetic dipoles the line shape is Lorentzian. More recently this theory has been shown to apply to the *intrinsic* linewidth for paramagnetic ions diluted in a glass matrix.[27] If the linewidth is not very small in comparison with the resonance magnetic field B_0, instead of the Lorentzian line shape a *modified* Bloch line shape including both resonant (Larmor) and nonresonant (anti-Larmor) terms must be used:[28]

$$F(B_r,\Delta_B) = \frac{1}{3\sqrt{3}\pi\Delta_B^3}\left(\frac{B_r - B}{\left[1+\frac{1}{3}(B_r-B)^2/\Delta_B^2\right]^2} - \frac{B_r + B}{\left[1+\frac{1}{3}(B_r+B)^2/\Delta_B^2\right]^2}\right). \quad (9)$$

In the narrow line limit, $\Delta_B \ll B_r$, the linewidth parameter tends to the peak-to-peak half-width of a Lorentzian derivative-of-absorption curve.

In the actual case the magnetic susceptibility data, *vide ultra*, clearly show that the Gd1 glass contains only isolated Gd^{3+} ions, and the EPR data for the less-doped glasses (Gd1 and Gd2) indicate no appreciable dipole-dipole broadening. So, as a working hypothesis, we assume that the spin-Hamiltonian parameters governing the EPR spectra in the Gd3 and Gd4 glasses are the same as in Gd1; however, the *intrinsic* EPR lines are broadened by dipole-dipole interactions between the Gd^{3+} ions.

The numerical analysis of the EPR spectra includes three stages. At the first stage, the experimental EPR spectrum of the Gd1 glass measured at some temperature is integrated to obtain the "experimental" $\mathcal{J}(B_r)$ curve. At the second stage we produce a convolution of this curve with a derivative-of-absorption line shape conforming to Eq. (8). This "intermediate" spectrum features the contribution of Gd^{3+} ions diluted in the glass matrix to the total EPR spectrum of more heavily doped glasses. Finally, at the third stage, by subtracting this spectrum from the experimental EPR spectrum of the corresponding glass taken at the same temperature, we get a "difference" spectrum describing the contribution of nonisolated (clustered) Gd^{3+} ions.

The procedure outlined above is carried out by a trial-and-error method with two adjustable parameters: (i) the convolution linewidth used in computing the intermediate spectrum and (ii) the statistical weight of this spectrum in the experimental spectrum of a heavily doped glass. The criteria of the fitting are (i) the most satisfactory reproduction of the characteristic low-field EPR spectra features and (ii) the requirement that the difference spectrum should have the shape of a derivative-of-absorption EPR signal.

Surprisingly, we have found that this procedure yields consistent results only within a very restrained range of the adjustable parameter values. As a result, the error margins of the data shown in Table I could be determined.

The results of such fitting for the Gd4 glass are illustrated in the left parts of Figs. 5 and 6, respectively, for room and liquid helium temperatures. One can immediately see that the curves (b) calculated at the second stage and representing the contribution of isolated ions (in the sense of absence of clustering) do not satisfactorily reproduce the experimental spectra. Therefore, the spectra transformations with the concentration of the Gd^{3+} ions cannot be ascribed exclusively to the dipole-dipole broadening. This confirms our earlier conclusion reached using computer-generated theoretical spectra.[11]

On the other hand, taking into account the existence of an underlying resonance [curve (c), see the figure legends for the simulation parameters], the overall shape of the EPR spectra in Gd3 and Gd4 can be satisfactorily reproduced. The latter resonance is broad and featureless, and can be ascribed to clusters of Gd^{3+} ions. The structure of EPR spectra of the clusters is supposed to be smeared out by strong dipole-dipole interaction as well as exchange coupling between closely spaced Gd^{3+} ions.

The linewidths of the signals ascribed to diluted Gd^{3+} ions, curves (b) in Figs. 5 and 6 are given in Table II. Figure 7 shows the *squares* of these linewidths versus the Gd_2O_3 content. In spite of the small number of points, the proportionality between Δ_B and the square root of the concentration is clearly observed, as expected for diluted (in the sense of absence of exchange interactions) paramagnetic ions at intermediate doping levels.[27,29]

The shape of the underlying resonance in the high (between room and liquid nitrogen) and low (from about 50 K down to the liquid helium) temperatures is manifestly different, cf. the right parts of Figs. 5 and 6. In the first case the

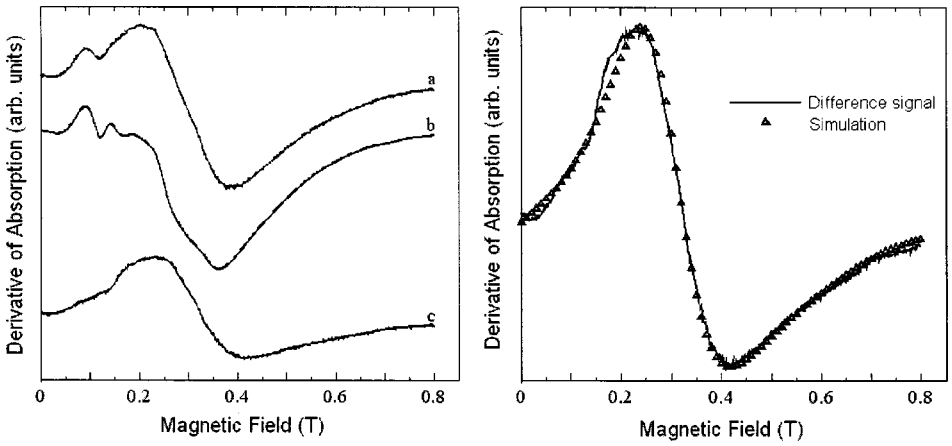

FIG. 6. Left: representation of the EPR spectrum of Gd4 at 4.5 K (a) as a linear combination of the liquid helium temperature spectrum of Gd1 convoluted with the line shape Eq. (9) for $\Delta_B = 0.010$ T (b) and an underlying resonance: (c)=(a)−0.55 (b). Right: fitting to the curve (c) with a superparamagnetic resonance signal (see the main text for the simulation parameters).

shape of this resonance can be convincingly fitted by a single "modified Bloch" line; see Eq. (9) with $B_r = 0.30$ T, corresponding to the effective g factor, $g_{eff} \approx 2.25$ and $\Delta_B = 0.10$ T; see Fig. 6, right.

A more complex situation occurs at low temperatures when the underlying resonance becomes clearly asymmetric; see Fig. 6. The shape of this spectrum is very similar to the superparamagnetic resonance spectrum observed for ferromagnetic $\gamma - Fe_2O_3$ nanoparticles in heat-treated sol-gel silica glass.[30] So, we have attempted to computer simulate this signal following the procedure outlined in this work.

For an isotropic intrinsic linewidth (in the actual case the question is the resonance width arising from particles of a given size and shape), the basic equations for calculating the superparamagnetic resonance spectrum have the same form as for the EPR; see above, Eqs. (7) and (8). Meanwhile the distribution density $P(\boldsymbol{X})$ in this case refers to size and shape characteristics of the nanoparticles.[24,30]

The energy density of magnetic nanoparticles is expressed as

$$E = -\boldsymbol{M}\cdot\boldsymbol{B}_r + K_1 F(\vartheta_M, \varphi_M) + \tfrac{1}{2}\mu_0 \boldsymbol{M}\cdot\mathbf{N}\cdot\boldsymbol{M}, \qquad (10)$$

with the three terms on the right-hand side representing the Zeeman energy, the magnetocrystalline anisotropy, and the magneto-static energy, respectively; K_1 is the first-order anisotropy constant, $F(\vartheta_M, \varphi_M)$ describes the magnetic symmetry with ϑ_M, φ_M the polar and azimuthal angles of the magnetization vector $\boldsymbol{M}$, and $\mathbf{N}$ is the demagnetizing tensor. The reduction of the thermal fluctuations of the nanoparticle magnetic moments reduces the angular anisotropy.

The resonance magnetic field is calculated by iteration from the following relation:

$$B_0 = \frac{1}{M \sin\vartheta_0}\left(\frac{\partial^2 E}{\partial\vartheta_M^2}\frac{\partial^2 E}{\partial\varphi_M^2} - \frac{\partial^2 E}{\partial\vartheta_M\,\partial\varphi_M}\right)^{1/2}\Bigg|_{\vartheta_M=\vartheta_0,\varphi_M=\varphi_0}, \qquad (11)$$

where $B_0 = \omega/\gamma$, ω is the microwave frequency and γ is the gyromagnetic ratio. The derivatives in Eq. (11) are calculated for angles ϑ_0 and φ_0 minimizing the value of E.

In a system of nanoparticles *thermal fluctuations* of their magnetic moments severely reduce the anisotropy of the resonance magnetic field, resulting in superparamagnetic spectra narrowing. This reduction is more pronounced the smaller the particle volume V. For an assembly of particles whose magnetic moments are much larger than the Bohr magneton, the partition function can be calculated as an integral over all possible values of the angle between $\boldsymbol{M}$ and $\boldsymbol{B}_r$, $\vartheta = \vartheta_M - \vartheta_B$. In this approximation the magnetization and the magnetic anisotropy can be averaged over the thermal fluctuations of the magnetic moment, *viz.*, $\langle M\rangle = M\langle\cos\vartheta\rangle$ and $\langle K_1\rangle = K_1\langle P_n(\cos\vartheta)\rangle$ (the nth-order Legendre polynomial). The average values are expressed as functions of $x = MB_rV/kT$, *viz.*, $\langle\cos\vartheta\rangle = L(x) = \coth x - 1/x$ (the Langevin function) and, for axial symmetry ($n=2$), $\langle P_2(\cos\vartheta)\rangle = 1 - 3L(x)/x$.[31,32]

Since, in the actual case, magnetic parameters of the hypothetical ferromagnetic nanoparticles are not known, we have rather arbitrarily assumed the saturation magnetization value of $M_s = 5\times10^5$ A m^{-1} and axial magnetocrystalline anisotropy. Under this assumption, the following parameters could be deduced from the fitting to the low-temperature underlying resonance in Gd4: the magnetic anisotropy constant $K_1 = -10$ kJ m^{-3} (including contribution of both the magnetocrystalline anisotropy and particle shape anisot-

TABLE II. Estimates of intrinsic resonance widths Δ_B for isolated Gd^{3+} ions and clustering degree (K) in the glasses containing Gd (EPR data).

	Gd1		Gd2		Gd3		Gd4	
T (K)	77–300	4.2	77–300	4.2	77–300	4.2	77–300	4.2
Δ_B (mT)	<0.1	<0.1	<0.3	<0.3	7.0±0.5	6.0±0.5	10±0.1	10±0.1
K (%)	⋯	⋯	⋯	⋯	24±5	28±5	42±8	40±10

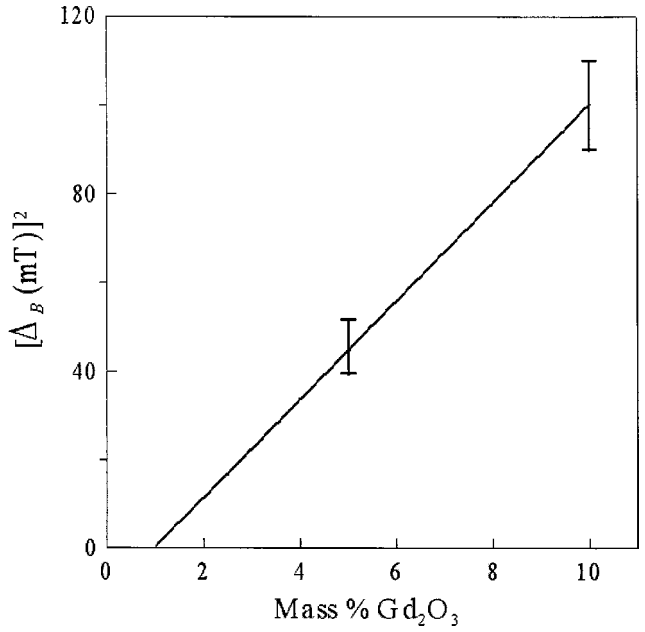

FIG. 7. Square of the intrinsic linewidth for isolated Gd^{3+} ions as a function of the Gd_2O_3 content. The straight line represents the linear regression $Y=11.09X-10.6$.

ropy); the average diameter of 1 nm and the distribution width (for the log-normal diameter distribution) 0.2; an isotropic intrinsic line shape given in Eq. (9) with the linewidth parameter $\Delta_B=0.065$ T. The parameter values estimated for Gd3 are close to those quoted for Gd4.

We note a persistent discrepancy between the shape of the experimental resonance curves due to clusters and the corresponding theoretical spectra in the low-magnetic field range. This discrepancy cannot be removed by any choice of such fitting parameters as linewidth and the relative intensity of the underlying resonance. Therefore, this shows that certain modifications in the spin-Hamiltonian parameter values occur as the gadolinium contents in the glasses increases. These modifications are indicative of different ordering degrees in the glass matrix at different doping levels.

From the above analysis the fraction of clustered Gd^{3+} ions in the glasses can be evaluated as the relative intensity of the underlying resonance with respect to that of the total EPR spectrum. This fraction, obtained by double integration of the corresponding derivative-of-absorption spectra, is shown in Table II.

Interestingly, a significant disagreement is noted between the estimations of the clustering degree from the susceptibility and EPR measurements (cf. Tables I and II). This disagreement can be explained by different contributions of clusters of different size into static susceptibility, on the one hand, and to the EPR spectra, on the other hand. Vonsovskii[33] put forward the following model, later confirmed by many authors, for example, see Refs. 34 and 35. Because of the quantum character of the cooperative ferromagnetism, magnetic ordering at nonzero temperature occurs only if the cluster size exceeds some critical value. According to the Heisenberg relation, the impulse p of an electron moving freely inside a system of linear dimension δ_0 has an uncertainty

$$\Delta p \approx \hbar/\delta_0. \tag{12}$$

The corresponding electron zero energy Δ_{ε_0}, arising from the fact that an electron "feels" the boundaries of the system where it is confined, is

$$\Delta_{\varepsilon_0} \approx \Delta p^2/2m \approx \hbar^2/2m\delta_o^2. \tag{13}$$

Numerically, for m equal to the free-electron mass, we get

$$\Delta_{\varepsilon_0} \approx 10^{-27}/\delta_0^2. \tag{14}$$

Comparing this energy to the exchange energy $A \approx k\Theta$, we can determine the critical particle size below which ferromagnetism vanishes at any temperature. Usually this size is of an order of several interatomic distances. The existence of the magnetic order in a cluster at nonzero temperature is of importance for the field and temperature dependencies of the static susceptibility. So, only clusters of larger size give predominant contributions to the static susceptibility, while in the case of the EPR spectra the contributions of clusters of any size (ordered or nonordered) are comparable. Thus, this model explains the difference between the fractions of clustered Gd ions in the Gd3 and Gd4 samples obtained with the two techniques.

The situation is more complex for the Gd2 glass. In the range between room- and liquid-nitrogen temperatures its EPR spectra are very similar to those of Gd1, so that neither line broadening nor trace of underlying resonance can be detected for the former glass. At liquid helium temperature the spectrum of Gd2 becomes different from that of Gd1. We attempted to apply the same analysis as in the case of Gd3 and Gd4 glasses. Meanwhile, no distinct manifestation of clustering could be detected by EPR in this case. Possibly, this can be explained by the low Gd content in combination with the low fraction of ions included in clusters (Table I) in this sample.

C. Optical absorption

The optical absorption spectra shown in Fig. 8 are markedly different for Gd1 and all other glasses. In the first case, the absorption is due to the basic glass components and La; the gadolinium contribution is negligible because of its low content. In the second case, the presence of Gd^{3+} manifests itself in an absorption edge shift to lower energies, a shoulder in the region of $\sim(35\text{–}45)\times10^3$ cm^{-1} and in weak narrow line sets centered at approximately 32, 36, and 40 $\times10^3$ cm^{-1}. The latter are identified as f-f transitions within the Gd^{3+} ions, respectively, $^8S_{7/2}\rightarrow{}^6P_J$, $^8S_{7/2}\rightarrow{}^6I_J$, and $^8S_{7/2}\rightarrow{}^6D_J$. Because of a low transparency of the glasses, the high-energy parts of the absorption curves can be obtained only in a narrow spectral range; nevertheless, they clearly show the onset of the fundamental absorption band. In this range the absorption coefficient is approximately a linear function of the photon energy, and its extrapolation to the intersection with the energy axis gives a rough estimate of the absorption band edge E_g as $\sim44\times10^3$ and ~42 $\times10^3$ cm^{-1} for Gd1 and Gd2–Gd4, respectively. The red E_g shift with the increased Gd concentration correlates with the clustering of Gd. This correlation can be accounted for by

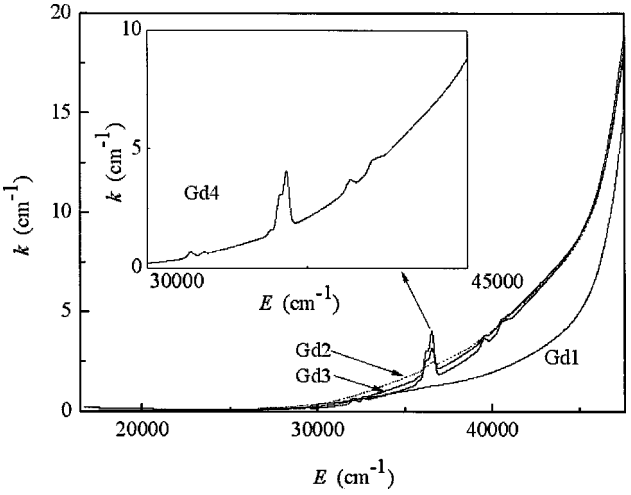

FIG. 8. Absorption coefficient k for Gd1–Gd4 glasses at room temperature. The inset shows the region of the f-f transitions for Gd4 glass.

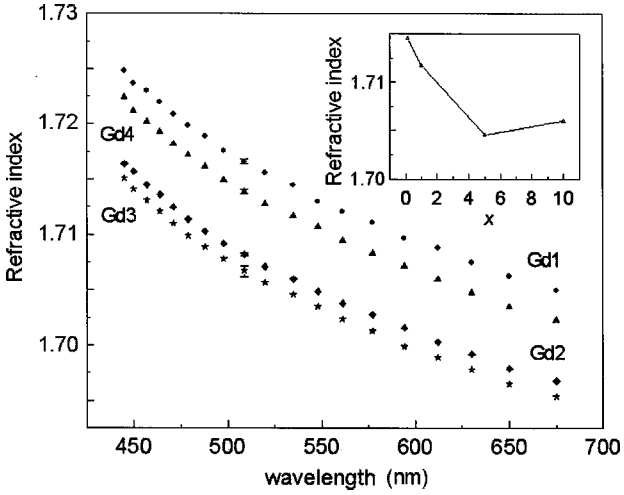

FIG. 10. Refractive index versus the light wavelength. Inset: dependence of the refractive index on the Gd_2O_3 concentration (x).

charge transfer transitions Gd-Gd, in the clusters.

A part of the f-f spectrum in the region of $^8S_{7/2} \rightarrow {}^6I_J$($36 \times 10^3$ cm^{-1}) is shown in Fig. 9. Three components $^8S_{7/2} \rightarrow {}^6I_{7/2}$ (35 715 cm^{-1} for Gd2 and 35 775 cm^{-1} for Gd3 and Gd4, correspondingly); $\rightarrow({}^6I_{9/2}, {}^6I_{17/2})$ (36 160 cm^{-1} for Gd2 and 36 165 cm^{-1} for Gd3 and Gd4); and $\rightarrow({}^6I_{11/2}, {}^6I_{13/2}, {}^6I_{15/2})$ (36 495 cm^{-1} for all samples) are resolved in this region, similar to Gd^{3+} spectra in borate[36] and alkali-zinc-boron-sulphate[37] glasses, while in glasses and compounds based on fluorine or chlorine, four lines are usually resolved (see, for instance, Refs. 38–40). Energies and oscillator strengths of the components as a function of the Gd concentration were analyzed in detail previously,[11] and small changes of these characteristics were shown to take place when coming from Gd2 to Gd3 or Gd4 glasses. The main difference between Gd2 and Gd3 (Gd4) is a shift towards higher energies of the transition between levels with the *same J* value, $^8S_{7/2} \rightarrow {}^6I_{7/2}$. This difference, though minor, was beyond the errors of the measurements, so it was indicative of certain changes in the Gd^{3+} environment arising with the increase of the Gd_2O_3 content. Energies of f-f transitions in compounds (in contrast to d-d transitions) usually depend only on crystal field (CF), but not on covalence (nephelauxetic effect), and, as a rule, they are higher for lower CF. So, one can suppose CF in Gd3 and Gd4 to be weaker than in Gd2. The CF strength reduction can be due to substitution of La for Gd. Both smaller Gd^{3+} ion radius (0.94 Å) in comparison with La^{3+} radius (1.04 Å) and possible change of the glass structure at higher Gd content can be responsible for the CF strength reduction.

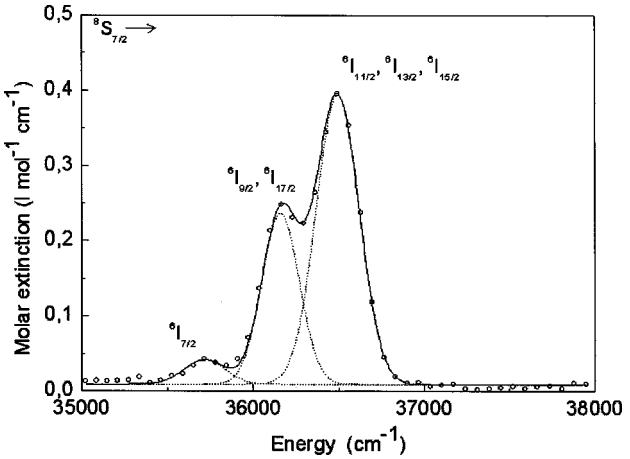

FIG. 9. Absorption spectrum in the region of $^8S_{7/2} \rightarrow {}^6I_J$ transitions and decomposition of this band into three lines, in agreement with the observed spectra features for the Gd3 sample at 300 K. The circles are experimental points and the solid line is the sum of the three components shown by the dashed lines.

Figure 10 shows spectral dependencies of the refraction index (n). Nonmonotonous n decrease with the Gd content (x) increase attracts one's attention (inset in Fig. 10). Contrary to the absorption, which reflects, first of all, the closest surroundings of RE ions and these ions' interaction, the refractive index evidences, in the higher extent, some changes in the glass structure when x changes from 1.0 to 10.0 mass %. A similar break in the refractive index dependence versus x was observed in Ref. 7, which was ascribed to a structural change occurring in the glass matrix. If we suppose that clusters of two different types (with ferromagnetic and antiferromagnetic exchange interaction between Gd ions) are formed in the glasses investigated, the change of glass structure with the Gd content increase can explain the change of the relative quantity of these clusters in dependence on x and the reduction of the paramagnetic Curie temperature for the higher Gd content.

IV. SUMMARY

We have observed a complex magnetic behavior in the glasses $\{xGd_2O_3-(20-x)La_2O_3-22Al_2O_3-23B_2O_3-35(SiO_2+GeO_2)\}$. The magnetic susceptibility χ follows the Curie-Weiss low with positive Weiss constant Θ; besides, the latter decreases with an increase of x. To elucidate this uncommon situation we have analyzed the results observed

using the function $\chi T = f(T)$. Two peculiarities were revealed: at 55 K and at 12 K. The former feature was ascribed to a ferromagnetic and the latter one to an antiferromagnetic phase transitions in Gd clusters of two types. The computer-assisted EPR study reveals gadolinium clustering in heavily doped glasses and magnetic ordering at low temperatures. In addition, it indicates certain modifications in the ordering degree in the glass matrix at different doping levels. The shift of the strong absorption band edge as a function of Gd concentration correlates with the beginning of the Gd cluster formation and is accounted for by Gd-Gd charge transfer transitions in the clusters. The dependencies of the f-f absorption band's characteristics and the refractive index on the Gd concentration (x) testify to changes of the Gd surroundings and glass structure with x change.

ACKNOWLEDGMENTS

The work was supported by the Krasnoyarsk Regional Science Foundation, Grant No. 12F0045C. One of us (A.M.) acknowledges financial support from the Israeli Ministry of Absorption.

*Electronic address: ise@iph.krasn.ru

[1] M. Rotter, M. Loewenhaupt, M. Doerr, A. Lindbaum, H. Sassik, K. Ziebeck, and B. Beuneu, Phys. Rev. B **68**, 144418 (2003).
[2] C. J. Schinkel and W. D. Van Amstel, Phys. Lett. **44A**, 467 (1973).
[3] R. M. Moon and W. C. Koehler, Phys. Rev. B **11**, 1609 (1975).
[4] B. Antic, M. Mitric, D. Rodic, Y. Zhong, Y. Artemov, S. Bogdanovich, and J. R. Friedman, Phys. Rev. B **58**, 3212 (1998).
[5] S. S. Simon, R. Pop, V. Simon, and M. Coldea, J. Non-Cryst. Solids **331**, 1 (2003).
[6] I. Ardelean, E. Burzo, D. Mitulescu-Ungar, and S. Simon, J. Non-Cryst. Solids **146**, 256 (1992).
[7] E. Culea and I. Milea, J. Non-Cryst. Solids **189**, 246 (1995).
[8] E. Culea, A. Pop, and I. Cosma, J. Magn. Magn. Mater. **157/158**, 163 (1996).
[9] T. Ristoiu, E. Culea, and I. Bratu, Mater. Lett. **41**, 135 (1999).
[10] S. Simon, I. Ardelean, and S. Filip, I. Bratu, and I. Cosma, Solid State Commun. **116**, 83 (2000).
[11] J. Kliava, I. S. Edelman, A. M. Potseluyko, E. A. Petrakovskaja, R. Berger, I. Bruckental, Y. Yeshurun, A. V. Malakhovskii, and T. V. Zarubina, J. Phys.: Condens. Matter **15**, 6671 (2003).
[12] R. L. Carlin, *Magneto-chemistry* (Springer-Verlag, Berlin, Heidelberg, 1986).
[13] G. C. DeFotis, F. Palacio, and R. L. Carlin, Phys. Rev. B **20**, 2945 (1979).
[14] S. H. Yuan and S. M. Chee, J. Appl. Phys. **70**, 6272 (1991).
[15] T. Ohtani, B. Chevalier, P. Lejay, J. Etourneau, M. Vlasse, and P. Hagenmuller, J. Appl. Phys. **54**, 5928 (1983).
[16] A. E. Miller, F. J. Jelinek, K. A. Gschneidner, and B. C. Gerstein, Jr., J. Chem. Phys. **55**, 2647 (1971).
[17] S. V. Vonsovskii, *Magnetism* (Wiley, New York, 1974), Vol. 2, p. 969.
[18] D. H. Martin, *Magnetism in Solids* (MIT Press, Cambridge, MA, 1967).
[19] R. L. Carlin, L. J. Lambrecht, and H. J. Claus, J. Appl. Phys. **53**, 2634 (1982).
[20] A. V. Malakhovskii, I. S. Edelman, Y. Radzyner, Y. Yeshurun, A. M. Potseluyko, T. V. Zarubina, A. V. Zamkov, and A. I. Zaitzev, J. Magn. Magn. Mater. **263**, 161 (2003).
[21] C. M. Brodbeck and L. E. Iton, J. Chem. Phys. **83**, 4285 (1985).
[22] L. Cugunov, A. Mednis, and J. Kliava, J. Phys.: Condens. Matter **3**, 8017 (1991).
[23] C. B. Azzoni, D. Martino, A. Paleari, A. Speghini, and M. Bettinelli, J. Mater. Sci. **34**, 3931 (1999).
[24] J. Kliava and R. Berger, in *Recent Res. Devel. Non-Crystalline Solids* (Transworld Research Network, Kerala, 2003), Vol. 3, pp. 41–84.
[25] J. Kliava, *EPR Spectroscopy of Disordered Solids* (Zinatne, Riga, 1988) (in Russian).
[26] J. H. Van Vleck, Phys. Rev. **74**, 1168 (1948).
[27] R. Berger, J. Kliava, E.-M. Yahiaoui, J.-C. Bissey, P. K. Zinsou, and P. Beziade, J. Non-Cryst. Solids **180**, 151 (1995).
[28] R. Berger, J.-C. Bissey, and J. Kliava, J. Phys.: Condens. Matter **12**, 9347 (2000).
[29] C. Kittel, and E. Abrahams, Phys. Rev. **90**, 238 (1953).
[30] J. Kliava and R. Berger, J. Magn. Magn. Mater. **205**, 328 (1999).
[31] R. S. de Biasi and T. C. Devezas, J. Appl. Phys. **49**, 2466 (1978).
[32] Yu. L. Raikher and V. I. Stepanov, Sov. Phys. JETP **75**, 764 (1992).
[33] S. V. Vonsovskii, Izv. Akad. Nauk SSSR, Ser. Phys **16**, 387 (1952).
[34] S. Shtrikman and D. Treves, in *Magnetism*, edited by G. T. Rado and H. Suhl (Academic, New York, 1963), Vol. III.
[35] E. Kneller, in *Handbuch der Physik*, edited by H. P. J. Wijn (Springer-Verlag, Berlin, 1966), Bd.18/2, p. 438.
[36] J. W. M. Verwey, G. F. Imbusch, and G. Blasse, J. Phys. Chem. Solids **50**, 813 (1989).
[37] B. Sreedhar, J. Lakshmana Rao, G. L. Narendra, and S. V. J. Lakshman, J. Phys. Chem. Solids **59**, 67 (1992).
[38] H. H Caspers, S. A. Miller, H. E. Rast, and J. L. Fry, Phys. Rev. **180**, 329 (1969).
[39] E. M. Stephens, D. H. Metcalf, M. T. Berry, and F. S. Richardson, Phys. Rev. B **44**, 9895 (1991).
[40] K. Binnemans, C. Gorller-Walrand, and J. L Adam, Chem. Phys. Lett. **280**, 333 (1997).